SB^{3}C2020
Summer Biomechanics, Bioengineering and Biotransport Conference
June 17-20, Vail, CO, USA

A 3-D CONSTITUTIVE MODEL FOR FINITE ELEMENT ANALYSES OF AGAROSE WITH A RANGE OF GEL CONCENTRATIONS

Xiaogang Wang (1), Ronald K. June (2), David M. Pierce (1,3)

(1) Department of Mechanical Engineering
University of Connecticut
Storrs, CT, USA

(2) Department of Mechanical and Industrial Engineering
Montana State University
Bozeman, MT, USA

(3) Department of Biomedical Engineering
University of Connecticut
Storrs, CT, USA

INTRODUCTION

Agarose is a cell-compatible hydrogel with broad applications in mechanobiology and tissue engineering. Several studies have recently utilized agarose to create 3-D cellular microenvironments. Advances in the preparation of agarose gels enable successful encapsulation of viable cells at gel concentrations of 4.5% which result in equilibrium moduli of ~35 kPa. Cartilage, a soft tissue that lines the surfaces of joints, is synthesized by chondrocytes which reside within the pericellular matrix (PCM) of cartilage. The stiffness of PCM is between 25-100 kPa. Therefore, agarose can serve as an experimental model mimicking the 3-D microenvironment of the PCM in cartilage *in vivo*.

Finite-element-based computational models allow researchers to better understand the specific 3-D mechanical microenvironment during mechanical stimulation, and to compare specific stress, strain, or pressure measures with cell-driven mechanobiological results. However, 3-D constitutive models of high-stiffness agarose are currently unavailable. In this study we aimed to establish a 3-D constitutive model of high-stiffness agarose with concentrations of 3-5%. The model and the fitted parameters enable more precise finite element (FE) simulations, and thus better understanding of experiments aimed at mechanobiology and tissue engineering of cartilage.

METHODS

Agarose Constructs. We prepared constructs for mechanical testing using low-gelling-temperature agarose (Sigma: Type VII-A A0701). We dissolved 3–5% (w/v) agarose in phosphate-buffered saline (PBS) at 1.1× strength and 40°C. After ~5 min we diluted dissolved agarose to 1× with 40°C PBS. We cast agarose in anodized aluminum molds at 23°C producing cylindrical constructs (height: 12.7 ± 0.1 mm; diameter: 7.0 ± 0.1 mm; determined using >20 independent constructs) which could encapsulate cells [1]. The construct geometry provides a homogeneous mechanical strain during uniaxial compression.

Mechanical Testing. We used a custom-built bioreactor to apply displacement-controlled loadings with sub-micron precision. Prior to testing, we equilibrated constructs in PBS at 37°C for 30 min. We then applied unconfined, uniaxial compression along the main axis using four consecutive steps of 4% nominal compressive Lagrange strain, and we held each strain step for 90 min at 37°C in tissue culture conditions (humidified 5% CO2 atmosphere). We sampled time, displacement, and force at 1000 Hz for the duration of each test.

Finite Element Model. We modeled one quarter of the cylindrical constructs using 20-node hexahedra in FEBio (U. of Utah), Fig. 1. We applied symmetry boundary conditions to recreate the construct, fixed the nodes of the bottom surface in all degrees-of-freedom, and allowed interstitial fluid to drain only through the sides of the cylinder. We then applied stepwise, uniaxial compression to the nodes of the top surface.

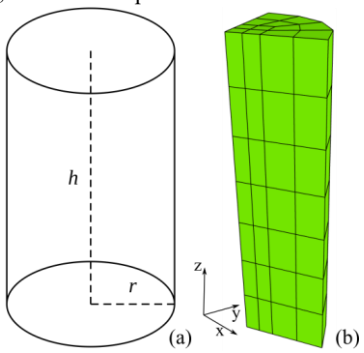

Figure 1: Finite element model: (a) cylindrical shape of the constructs (h = 12.7 mm, r = 7.0 mm); (b) corresponding mesh.

Constitutive Model. We described agarose gel as a biphasic continuum $\varphi = \varphi^{\mathrm{S}} + \varphi^{\mathrm{F}}$ consisting of a solid phase φ^{S}, with an isotropic and statistically regular pore distribution, and saturated with the fluid phase φ^{F}. We calculated the total Cauchy stress tensor as [2]

$$\boldsymbol{\sigma} = -p\mathbf{I} + \frac{2}{J_{\mathrm{S}}}\mathbf{F}_{\mathrm{S}}\frac{\partial \Psi^{\mathrm{S}}}{\partial \mathbf{C}_{\mathrm{S}}}\mathbf{F}_{\mathrm{S}}^{\mathrm{T}} = -p\mathbf{I} + \boldsymbol{\sigma}_{\mathrm{E}}^{\mathrm{S}}\,, \tag{1}$$

where p is the fluid pressure, $\mathbf{I}$ is the second-order identity tensor, $J_{\mathrm{S}} = \det \mathbf{F}_{\mathrm{S}}$ is the Jacobian, $\mathbf{F}_{\mathrm{S}} = \partial \mathbf{x}_{\mathrm{S}}/\partial \mathbf{X}_{\mathrm{S}}$ is the deformation gradient of the solid, $\mathbf{C}_{\mathrm{S}} = \mathbf{F}_{\mathrm{S}}^{\mathrm{T}}\mathbf{F}_{\mathrm{S}}$ is the right Cauchy–Green tensor, and $\boldsymbol{\sigma}_{\mathrm{E}}^{\mathrm{S}}$ is the effective Cauchy stress tensor. We assumed a Neo-Hookean constitutive model for the solid phase [3]

$$\Psi^{\mathrm{S}} = \frac{K}{2}(\ln J_{\mathrm{S}})^2 + \frac{\mu}{2}(I_1 - 3)\,, \tag{2}$$

where μ [Pa] is the shear modulus, K [Pa] is a bulk-modulus-like penalty parameter enforcing material incompressibility ($K > 1000\,\mu$).

We calculated the viscous contribution to the total stress using the second Piola-Kirchhoff effective stress $\mathbf{S} = \mathbf{S}_{\mathrm{E}}^{\mathrm{S}} = J\mathbf{F}_{\mathrm{S}}^{-1}\boldsymbol{\sigma}_{\mathrm{E}}^{\mathrm{S}}\mathbf{F}_{\mathrm{S}}^{-\mathrm{T}}$. We march through time $t \in [0+, T]$ and focus on a subinterval $[t_n, t_{n+1}]$, with $\Delta t = t_{n+1} - t_n$ the time increment. At times t_n and t_{n+1} we know all relevant kinematic quantities and calculate the stress $\mathbf{S}_n$ at time t_n. The second Piola–Kirchhoff stress $\mathbf{S}_{n+1}$ at time t_{n+1} is then

$$\boldsymbol{S}_{n+1} = \boldsymbol{S}_{n+1}^{\infty} + \boldsymbol{Q}_{n+1}\,, \tag{3}$$

where $\mathbf{S}_{n+1}^{\infty}$ is the total elastic response computed from the given strain measures at t_{n+1}. We then computed the non-equilibrium stresses

$$\mathbf{Q}_{n+1} = \beta\xi(\mathbf{S}_{n+1}^{\infty} - \mathbf{S}_n^{\infty}) + \xi^2\mathbf{Q}_n\,, \tag{4}$$

where β [-] is a dimensionless magnitude factor, $\xi = \exp(-\Delta t/2\tau)$, τ [s] is the associated relaxation time, and $\mathbf{Q}_0 = \mathbf{0}$ [4].

The associated constitutive model for the hydraulic permeability relates the seepage velocity $\mathbf{w}$ to the interstitial fluid pressure p according to $\mathbf{w} = -\mathbf{k}\cdot \operatorname{grad} p$, where $\mathbf{k}$ is the hydraulic permeability tensor. We used the isotropic Holmes-Mow permeability [5]

$$\mathbf{k} = k_0\left(\frac{J_{\mathrm{S}}n^{\mathrm{F}}}{n_0^{\mathrm{F}}}\right)^{\alpha} e^{\frac{1}{2}M(J_{\mathrm{S}}^2-1)}\mathbf{I}\,, \tag{7}$$

where k_0 [$\mathrm{m}^4/(\mathrm{N}\cdot\mathrm{s})$] is the reference hydraulic permeability, and α [-] and M [-] are dimensionless parameters controlling the deformation dependence of the permeability. We chose to fix $\alpha = 2$ and $M = 1.5$. We calculated k_0 with Darcy permeability κ [m^2] and dynamic viscosity μ_{v} [$\mathrm{Pa}\cdot\mathrm{s}$] by $k_0 = \kappa/\mu_{\mathrm{v}}$. For agarose with different concentrations we used [6]

$$\frac{\kappa}{a^2} = -\frac{3}{20\phi}(\ln\phi + 0.931)\,, \tag{8}$$

where a is the fiber radius and ϕ is the concentration of the agarose gel. We used $a = 1.9$ nm [7] and we obtained the viscosity of agarose gels with varying concentrations from previous studies [8], cf. Table 1.

Table 1: Permeability parameters of agarose gel with concentrations of 3-5%.

ϕ [%]	κ [mm^2]	μ_{v} [$\mathrm{MPa}\cdot\mathrm{s}$]	k_0 [$\mathrm{mm}^4/\mathrm{N}\cdot\mathrm{s}$]
3.0	4.648×10^{-11}	1.00×10^{-6}	4.65×10^{-5}
3.5	3.746×10^{-11}	1.75×10^{-6}	2.14×10^{-5}
4.0	3.097×10^{-11}	2.50×10^{-6}	1.24×10^{-5}
4.5	2.611×10^{-11}	3.25×10^{-6}	8.03×10^{-6}
5.0	2.236×10^{-11}	4.00×10^{-6}	5.59×10^{-6}

Fitting the Model. We filtered and resampled the experiment data. We optimized the model parameters using the "Levenberg-Marquardt" method within FEBio. We first ran the elastic simulations fitting only the shear modulus μ. Next, we fit the viscoelastic parameters, β and τ using the fitted μ. We captured the peak reaction forces at the start of each compression phase and the reaction forces every minute thereafter.

RESULTS

Figure 2 shows representative experiment data, filtered data, and results from an FE simulation with optimized parameters. Table 2 includes the results of parameter optimization from representative agarose gels from each concentration. The shear modulus μ increases, while β decreases and τ increases, as the concentration increases.

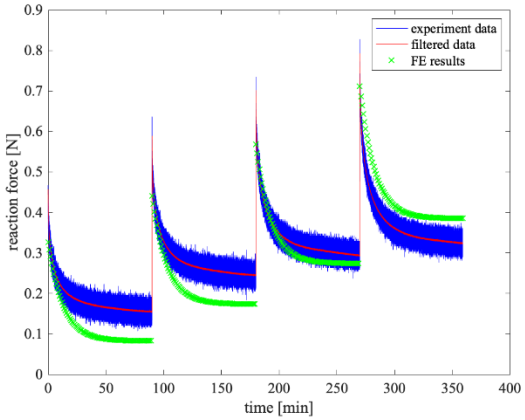

Figure 2: Representative experiment and FE simulation results.

Table 2: Parameters for agarose gels with concentrations of 3-5%.

ϕ [%]	μ [MPa]	β [-]	τ [s]
3.0	7.41×10^{-3}	3.44	430.22
3.5	9.57×10^{-3}	3.54	394.29
4.0	1.19×10^{-2}	3.38	622.60
4.5	1.29×10^{-2}	3.26	720.06
5.0	1.57×10^{-2}	3.08	763.86

DISCUSSION

The representative experimental data indicates that the agarose gel softens as the compression increases. However, the biphasic neo-Hookean model generally stiffens with increasing compression. Our simulations assume that the agarose gels remain isotropic under compression. However, agarose gels may contain fiber-like structures, which might affect the mechanical responses under compression [7].

Our two-step optimization separately fits different sets of model parameters and helps to achieve faster convergence. We are currently optimizing model parameters using experimental data from many more constructs and aim to generate statistically relevant distributions in these parameters. Using the fitted constitutive models will allow simulation of agarose gels of varying concentrations with the aim to better understand mechanobiological responses of agarose-encapsulated cells under arbitrary loading conditions.

ACKNOWLEDGEMENTS

NSF CAREER 1653358 and NIH 1R01AR073964-01A1.

REFERENCES

[1] Jutila, A. A. et al. Ann Biomed Eng, 43(5):1132-44, 2015
[2] Pierce, D. M. et al. *Biomech Model Mechanobiol*, 15:229-244, 2016.
[3] Simo J. C. et al. *Comput Meth Appl Mech Eng*, 46:201–215, 1984.
[4] Holzapfel, G. A. et al. *Comput Meth Appl Mech Eng*, 190:4379–4403, 2001.
[5] Holmes, M. H. et al. *J Biomech*, 23:1145-56, 1990.
[6] Johnson, E. M. et al. *AIChE Journal*, 42:1220-1224, 1996.
[7] Djabourov, M. et al. *Macromolecules*, 22(1):180-188, 1989.
[8] Fernández, E. et al. *J Polym Sci B Polym Phys*, 46(3):322-328, 2008.